Synchronization as adjustment of information rates: Detection from bivariate time series

Milan Paluš
Institute of Computer Science, Academy of Sciences of the Czech Republic, Pod vodárenskou věží 2, 182 07 Prague 8, Czech Republic

Vladimír Komárek, Zbyněk Hrnčíř, and Katalin Štěrbová
Clinic of Paediatric Neurology, 2nd Medical Faculty of Charles University, V úvalu 84, 150 06 Prague 5–Motol, Czech Republic

(Received 5 July 2000; revised manuscript received 4 December 2000; published 28 March 2001)

An information-theoretic approach for studying synchronization phenomena in experimental bivariate time series is presented. ''Coarse-grained'' information rates are introduced and their ability to indicate generalized synchronization as well as to establish a ''direction of information flow'' between coupled systems, i.e., to discern the driving from the driven (response) system, is demonstrated using numerically generated time series from unidirectionally coupled chaotic systems. The method introduced is then applied in a case study of electroencephalogram recordings of an epileptic patient. Synchronization events leading to seizures have been found on two levels of organization of brain tissues and ''directions of information flow'' among brain areas have been identified. This allows localization of the primary epileptogenic areas, also confirmed by magnetic resonance imaging and pasitron emission tomography scans.

DOI: 10.1103/PhysRevE.63.046211 PACS number(s): 05.45.Tp, 05.45.Xt, 89.70.+c

I. INTRODUCTION

During the last decade there has been considerable interest in the study of the cooperative behavior of coupled chaotic systems [1]. Synchronization phenomena have been observed in many physical and biological systems, even in cases where the chaotic nature of the scrutinized processes has not been proven or is in doubt, e.g., in the case of cardiorespiratory synchronization [2,3] or synchronization of neural signals [4–7]. In such physiological and neurophysiological systems it is important not only to detect synchronized states, but also to identify causal (drive-response) relationships between studied (sub)systems. Although several methods have been proposed and successfully applied, especially in the field of neurophysiology [4–7], this problem is far from being trivial and some claims of successful detection of the causal relationships are based on contradictory assumptions [4,5]. Also, measures of synchronization based on infinitesimal properties and performing well on artificial systems can fail when applied to noisy experimental data. We propose to start a study of synchronization in such data with statistical, coarse-grained measures with a basis in information theory, which could provide an indication of synchronization as well as of causal relationships if present in the systems scrutinized.

In Sec. II the definitions of entropy, information, and information rates are briefly reviewed. More details can be found, e.g., in Ref. [8]. Then, the concept of ''coarse-grained entropy rates,'' originally introduced in Ref. [12] is summarized and extended by defining the coarse-grained information rates (CIR's) and their mutual and conditional versions. In Sec. III the CIR's are applied to bivariate time series generated by unidirectionally coupled chaotic systems (Hénon maps, Rössler and Lorenz systems) in order to demonstrate how the CIR's can detect synchronization and drive-response relationships. An application of the approach introduced is demonstrated in Sec. IV by a case study of electroencephalogram (EEG) recordings of an epileptic patient. A conclusion is given in Sec. V.

II. COARSE-GRAINED INFORMATION RATES

Consider discrete random variables X and Y with sets of values Ξ and Υ, respectively, probability distribution functions (PDF's) $p(x)$ and $p(y)$, and joint PDF $p(x,y)$. The *entropy* $H(X)$ of a single variable, say X, is defined as

$$H(X) = -\sum_{x \in \Xi} p(x) \log p(x), \tag{1}$$

and the *joint entropy* $H(X,Y)$ of X and Y is

$$H(X,Y) = -\sum_{x \in \Xi} \sum_{y \in \Upsilon} p(x,y) \log p(x,y). \tag{2}$$

The *conditional entropy* $H(Y|X)$ of Y given X is

$$H(Y|X) = -\sum_{x \in \Xi} \sum_{y \in \Upsilon} p(x,y) \log p(y|x). \tag{3}$$

The average amount of common information, contained in the variables X and Y, is quantified by the *mutual information* $I(X;Y)$, defined as

$$I(X;Y) = H(X) + H(Y) - H(X,Y). \tag{4}$$

The conditional mutual information $I(X;Y|Z)$ of the variables X, Y given the variable Z is given as

$$I(X;Y|Z) = H(X|Z) + H(Y|Z) - H(X,Y|Z). \tag{5}$$

For Z independent of X and Y we have

$$I(X;Y|Z) = I(X;Y). \tag{6}$$

The entropy and information are usually measured in bits if the base of the logarithms in their definitions is 2; here we use the natural logarithm and therefore the units are called nats.

Now, let $\{X_i\}$ be a stochastic process, i.e., an indexed sequence of random variables. Its entropy rate [8]

$$h=\lim_{n\to\infty}\frac{1}{n}H(X_1,\ldots,X_n), \tag{7}$$

where $H(X_1,\ldots,X_n)$ is the joint entropy of the n variables $X_1,\ldots,X_n$ with the joint PDF $p(x_1,\ldots,x_n)$, is a measure of ''information creation'' by the process $\{X_i\}$, or the rate at which the process ''forgets'' its history. The entropy rate, in the case of dynamical systems called Kolmogorov-Sinai entropy (KSE) [9–11], is a suitable tool for quantification of the dynamics of systems or processes; however, possibilities of its estimation from experimental data are limited to a few exceptional cases [8,11,12]. Instead, Paluš [12] has proposed to compute ''coarse-grained entropy rates'' (CER's) as relative measures of information creation and of the regularity and predictability of studied processes.

Let $\{x(t)\}$ be a time series considered as a realization of a stationary and ergodic stochastic process $\{X(t)\},t=1,2,3,\ldots$. In the following we will denote $x(t)$ as x and $x(t+\tau)$ as x_τ. For defining the simplest form of CER we compute the mutual information $I(x;x_\tau)$ for all analyzed data sets and find a τ_{max} such that for $\tau'\geqslant\tau_{max}$ $I(x;x_{\tau'})\approx 0$ for all the data sets. Then we define the norm of the mutual information

$$||I(x;x_\tau)||=\frac{\Delta\tau}{\tau_{max}-\tau_{min}+\Delta\tau}\sum_{\tau=\tau_{min}}^{\tau_{max}}I(x;x_\tau) \tag{8}$$

with $\tau_{min}=\Delta\tau=1$ sample as the usual choice. The CER h^1 is then defined as

$$h^1=I(x,x_{\tau_0})-||I(x;x_\tau)||. \tag{9}$$

It has been shown that the CER h^1 provides the same classification of states of chaotic systems as the exact KSE [12]. Since usually $\tau_0=0$ and $I(x;x)=H(X)$, which is given by the marginal probability distribution $p(x)$, the sole quantitative descriptor of the underlying dynamics is the mutual information norm (8), which we will call the coarse-grained information rate (CIR) of the process $\{X(t)\}$ and denote by $i(X)$.

Now, consider two time series $\{x(t)\}$ and $\{y(t)\}$ regarded as realizations of two processes $\{X(t)\}$ and $\{Y(t)\}$ which represent two possibly linked (sub)systems. These two systems can be characterized by their respective CIR's $i(X)$ and $i(Y)$. In order to characterize an interaction of the two systems, in analogy with the above CIR, we define their mutual coarse-grained information rate (MCIR)

$$i(X,Y)=\frac{1}{2\tau_{max}}\sum_{\tau=-\tau_{max};\tau\neq 0}^{\tau_{max}}I(x;y_\tau). \tag{10}$$

Due to the symmetry properties of $I(x;y_\tau)$ the mutual CIR $i(X,Y)$ is symmetric, i.e., $i(X,Y)=i(Y,X)$.

Assessing the direction of coupling between the two systems, we ask how the dynamics of one of the processes, say $\{X\}$, is influenced by the other process $\{Y\}$. For a quantitative answer to this question we propose to evaluate the conditional CIR $i_0(X|Y)$ of $\{X\}$ given $\{Y\}$:

$$i_0(X|Y)=\frac{1}{\tau_{max}}\sum_{\tau=1}^{\tau_{max}}I(x;x_\tau|y), \tag{11}$$

considering the usual choice $\tau_{min}=\Delta\tau=1$ sample. Recalling Eq. (6) we have $i_0(X|Y)=i(X)$ for $\{X\}$ independent of $\{Y\}$, i.e., when the two systems are uncoupled. Since we prefer a measure that vanishes for uncoupled systems (although then it can acquire both positive and negative values), we define

$$i(X|Y)=i_0(X|Y)-i(X). \tag{12}$$

For another approach to a directional information rate let us consider the mutual information $I(y;x_\tau)$ measuring the average amount of information contained in the process $\{Y\}$ about the process $\{X\}$ in its future τ time units ahead (τ-future hereafter). This measure, however, could also contain information about the τ-future of the process $\{X\}$ contained in this process itself if the processes $\{X\}$ and $\{Y\}$ are not independent, i.e., if $I(x;y)>0$. In order to obtain the ''net'' information about the τ-future of the process $\{X\}$ contained in the process $\{Y\}$ we need the conditional mutual information $I(y;x_\tau|x)$. The latter measure can also be understood as an information-theoretic formulation of the Granger causality concept [13]. Also, recently Schreiber [14] has proposed a ''transfer entropy'' which in special cases is equivalent to $I(y;x_\tau|x)$.

Next, we sum $I(y;x_\tau|x)$ over τ as above,

$$i_1(X,Y|X)=\frac{1}{\tau_{max}}\sum_{\tau=1}^{\tau_{max}}I(y;x_\tau|x), \tag{13}$$

and, in order to obtain the ''net asymmetric'' information measure, we subtract the symmetric MCIR (10):

$$i_2(X,Y|X)=i_1(X,Y|X)-i(X,Y). \tag{14}$$

Using a simple manipulation we find that $i_2(X,Y|X)$ is equal to $i(X|Y)$, defined in Eq. (12). By using two different methods we have arrived at the same measure, which we will denote by $i(X|Y)$ and call the coarse-grained transinformation rate (CTIR) of $\{X\}$ given $\{Y\}$. It is the average rate of the net amount of information ''transferred'' from the process $\{Y\}$ to the process $\{X\}$, or, in other words, the average rate of the net information flow by which the process $\{Y\}$ influences the process $\{X\}$.

III. ANALYSIS OF DATA FROM COUPLED CHAOTIC SYSTEMS

Consider unidirectionally coupled Hénon maps, similar to those studied in [4,15], with equations

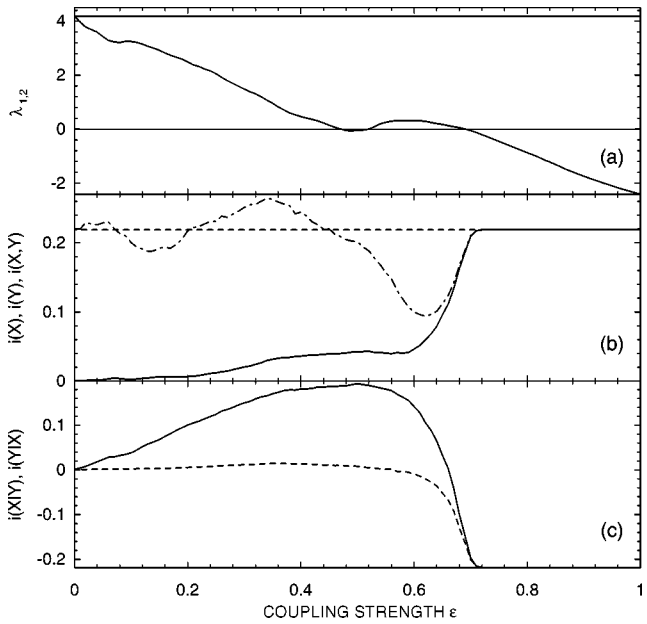

FIG. 1. (a) The largest Lyapunov exponents of the drive $\{X\}$ (constant line) and the response $\{Y\}$ (decreasing line), (b) the CIR $i(X)$ of the drive (dashed line) and $i(Y)$ of the response (dash-and-dotted line) and the mutual CIR $i(X,Y)$ (full line), (c) the coarse-grained transinformation rates $i(X|Y)$ (dashed line) and $i(Y|X)$ (full line) for the unidirectionally coupled identical ($b_1=b_2=0.3$) Hénon systems. The Lyapunov exponents are measured in nats per time unit; the CIR's in nats.

$$x_1' = 1.4 - x_1^2 + b_1 x_2,$$
$$x_2' = x_1 \tag{15}$$

for the driving system $\{X\}$, and

$$y_1' = 1.4 - [\epsilon x_1 y_1 + (1-\epsilon) y_1^2] + b_2 y_2,$$
$$y_2' = y_1 \tag{16}$$

for the response system $\{Y\}$. As the first example we use identical systems $b_1=b_2=0.3$. For 101 values of the coupling strength ϵ we iterate the systems (15),(16) and compute their Lyapunov exponents and all the coarse-grained information rates defined above. The latter are computed using simple box counting based on marginal equiquantization, i.e., a partition with equiprobable marginal bins [11,12,16]. The results, obtained using eight marginal bins, $\tau_{min}=\Delta\tau=1$, and $\tau_{max}=15$ samples, are illustrated in Fig. 1. The positive Lyapunov exponent (LE) of the drive is constant, while the largest LE of the response [LLE(Y) hereafter] decreases (although not monotonically) with increasing coupling strength ϵ [Fig. 1(a)], and for $\epsilon>0.7$ it remains negative, which is an indicator of a synchronized state (identical synchronization) [4]. The CIR $i(X)$ of the drive [the dashed line in Fig. 1(b)] is constant; the CIR $i(Y)$ of the response [dash-and-dotted line in Fig. 1(b)] is changing and becoming equal to $i(X)$ in the synchronized state. The mutual CIR $i(X,Y)$ [full line in Fig. 1(b)] is zero for small values of ϵ, starts to increase as LLE(Y) approaches zero, and finally

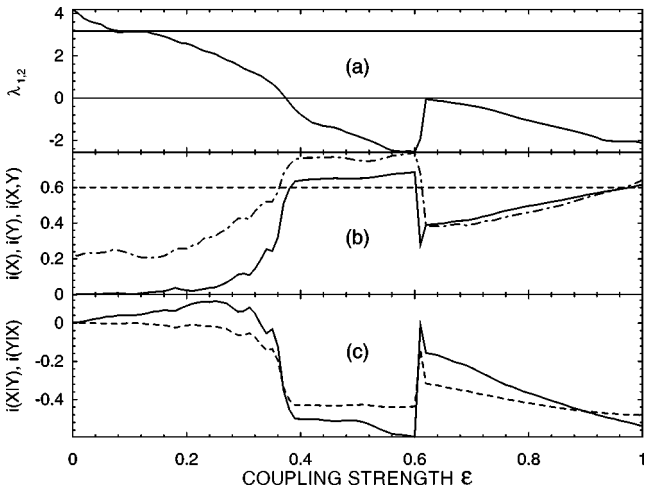

FIG. 2. The same as in Fig. 1 but for unidirectionally coupled nonidentical ($b_1=0.1$ and $b_2=0.3$) Hénon systems.

rises sharply at the synchronization threshold reaching the state of identical synchronization characterized by

$$i(X,Y) = i(X) = i(Y). \tag{17}$$

Note that before this triple equality is reached there is a state with $i(X,Y)=\min(i(X),i(Y))$.

The coarse-grained transinformation rates start at zero for $\epsilon=0$, then, with increasing ϵ the CTIR $i(Y|X)$ [full line in Fig. 1(c)] also increases to distinctly positive values while the CTIR $i(X|Y)$ [dashed line in Fig. 1(c)] remains zero. This result clearly indicates that the system $\{X\}$ drives the system $\{Y\}$, while $\{X\}$ evolves independently of $\{Y\}$. This distinction, however, ends shortly before the synchronization threshold, when both the CTIR's start to fall and reach the identical synchronization state with

$$i(X|Y) = i(Y|X) = -i(X) = -i(Y) = -i(X,Y).$$

With emerging synchronization we lose the possibility of establishing the direction of information flow, or the causal relationship between the systems $\{X\}$ and $\{Y\}$. It is understandable: in identical synchronization the series $\{x(t)\}$ and $\{y(t)\}$ are identical and there is no possibility of establishing the causal relationship between $\{X\}$ and $\{Y\}$ just from the data.

In the next example, consider nonidentical Hénon systems with $b_1=0.1$ and $b_2=0.3$. The positive LE [Fig. 2(a)] of the drive is again constant, while the largest LE of the response decreases with increasing ϵ and becomes negative at $\epsilon=0.38$. After $\epsilon=0.6$ it rises and touches zero around $\epsilon=0.62$ and then it falls again to negative values. Again, negative values of LLE(Y) define the synchronized states. Now we have an example of generalized synchronization [1,4,15] of two nonidentical systems. The CIR $i(X)$ [Fig. 2(b)] is constant, while $i(Y)$ reflects the development of LLE(Y). The mutual CIR $i(X,Y)$ is zero for $\epsilon<0.2$; it then rises with LLE(Y) approaching zero and then $i(X,Y)$ reflects the behavior of $i(Y)$. Since the CIR's, like their inspiration CER's [12], are not dynamical invariants, in the case of gen-

eralized synchronization we cannot expect the equality (17); however, the generalized synchronization is accompanied by $i(X,Y)$ rising to the values

$$\min(i(X),i(Y)) \leqslant i(X,Y) \leqslant \max(i(X),i(Y)). \qquad (18)$$

The CTIR's [Fig. 2(c)] indicate the correct causal relation of $\{X\}$ being a drive of $\{Y\}$ by their relation

$$i(X|Y) < i(Y|X), \qquad (19)$$

again only before the synchronization threshold. The above explanation of the impossibility of inferring a causal relation from identical time series in the state of identical synchronization can be generalized to time series related by a one-to-one nonlinear function, as is the case for generalized synchronization.

In the following example, consider the unidirectionally coupled Rössler and Lorenz systems described by the equations

$$\dot{x}_1 = -\alpha\{x_2 + x_3\},$$

$$\dot{x}_2 = \alpha\{x_1 + 0.2x_2\},$$

$$\dot{x}_3 = \alpha\{0.2 + x_3(x_1 - 5.7)\} \qquad (20)$$

for the autonomous Rössler system, and

$$\dot{y}_1 = 10(-y_1 + y_2),$$

$$\dot{y}_2 = 28y_1 - y_2 - y_1y_3 + \epsilon x_2^{\beta},$$

$$\dot{y}_3 = y_1y_2 - \tfrac{8}{3}y_3 \qquad (21)$$

for the driven Lorenz system in which the equation for $\dot{y}_2$ is augmented by a driving term involving x_2. First we analyze the case with $\alpha = 6$ and $\beta = 1$, also studied in [17]. The two LLE's of both systems are depicted in Fig. 3(a) (the constant positive and zero LE of the drive and partially decreasing LE of the response). After $\epsilon = 2$ the zero LE of the response becomes negative [Fig. 3(a), note the logarithmic scale], accompanied by a slight increase from zero values of the mutual CIR $i(X,Y)$ [Fig. 3(b)]. Then, between $\epsilon = 5$ and $\epsilon = 6$, LLE(Y) falls to zero and $i(X,Y)$ increases sharply so that for negative LLE(Y) the condition (18) for generalized synchronization is attained. The CTIR's start at zero values for small ϵ, then correctly reflect the causal relations by their inequality (19) which holds, again, only until the synchronized state is reached. The same behavior of the CIR's, MCIR, and CTIR's can be obtained for the case with $\alpha = 6$ and $\beta = 2$ (Fig. 4), also studied in [5,15].

In order to summarize the numerical study, we conclude that the above introduced CIR, MCIR, and CTIR can indicate synchronization [identical for the equality (17) and generalized for the relation (18)] and causal relations of drive and response (sub)systems [relation (19)]. The latter can be established only in states in which the (sub)systems are coupled, but not yet fully synchronized.

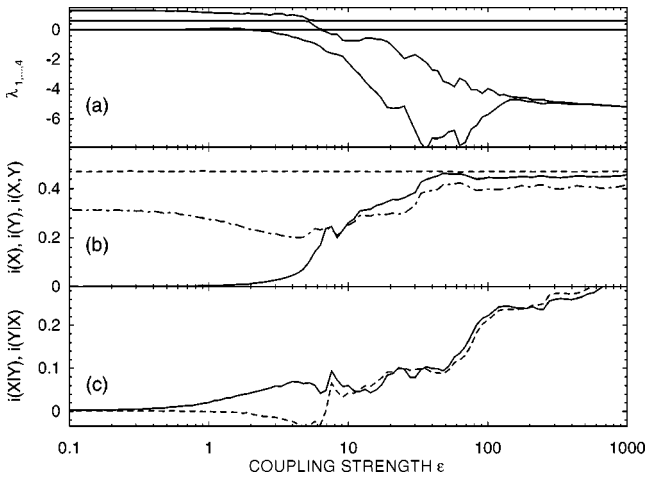

FIG. 3. (a) The two largest Lyapunov exponents of the drive $\{X\}$ (constant lines) and the response $\{Y\}$ (partially decreasing lines), (b) the CIR $i(X)$ of the drive (dashed line) and $i(Y)$ of the response (dash-and-dotted line) and the mutual CIR $i(X,Y)$ (full line), (c) the CTIR $i(X|Y)$ (dashed line) and $i(Y|X)$ (full line) for the Lorenz system $\{Y\}$ driven by the Rössler system $\{X\}$, $\beta = 1$. The Lyapunov exponents are measured in nats per time unit; the CIR's in nats.

IV. SYNCHRONIZATION AND INFORMATION FLOW IN THE EEG OF AN EPILEPTIC PATIENT

Synchronization on various levels of organization of brain tissue, from individual pairs of neurons to much larger scales—within one area of the brain or between different parts of the brain—is one of the most important topics in neurophysiology. Some level of synchrony is usually necessary in order to attain normal neural activity, while too much synchrony may be a pathological phenomenon such as epilepsy. Detection of synchrony, or transient changes leading to a high level of synchronization, and identification of causal relations between driving (synchronizing) and response (synchronized) components is a great challenge facing neurophysiologists and applied mathematicians and physicists, since it can help in anticipating epileptic seizures and in localization of epileptogenic foci. Standard linear sta-

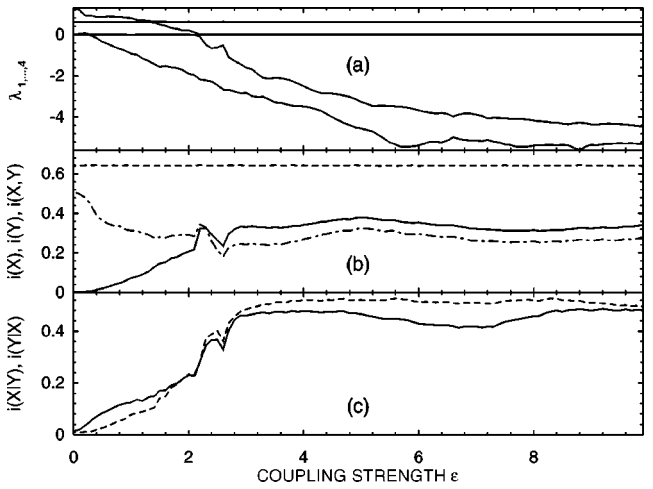

FIG. 4. The same as in Fig. 3, but for $\beta = 2$.

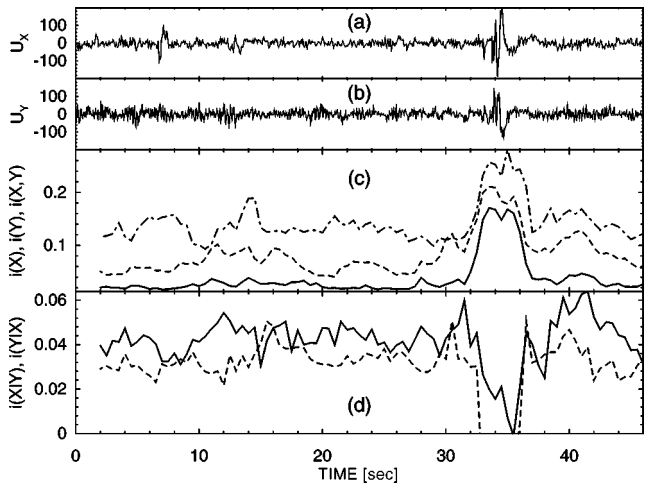

FIG. 5. (a) An EEG segment with a short seizure, recorded from leads T_6O_2 (a) and F_4C_4 (b). (c) The CIR's $i(T_6O_2)$ (dashed line) and $i(F_4C_4)$ (dash-and-dotted line) and the mutual CIR $i(T_6O_2,F_4C_4)$ (full line). (d) The coarse-grained transinformation rates $i(T_6O_2|F_4C_4)$ (dashed line) and $i(F_4C_4|T_6O_2)$ (full line). The EEG (brain potential), in practice measured in microvolts, is here presented in arbitrary units (bins of the analog-to-digital converter). The CIR's are in nats.

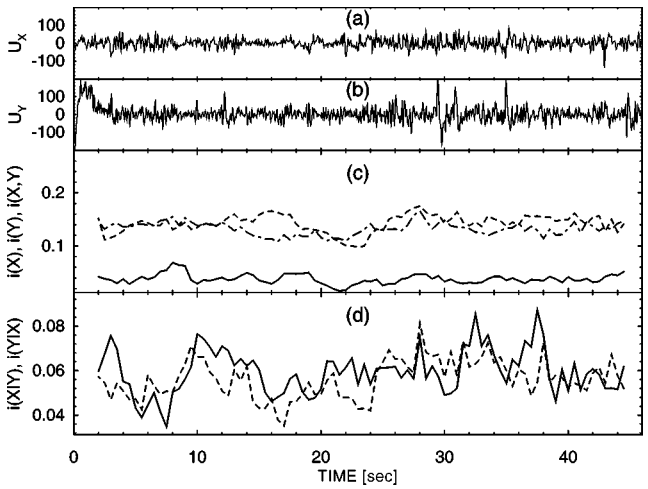

FIG. 6. The same as in Fig. 5, but for an interictal EEG segment.

tistical methods have brought only a little success in this area. Hope appeared in the field due to development of time series analysis methods that originated in studies of nonlinear dynamics, chaos, and chaotic synchronization [4–6,18,19]. Here we present a case study in which the coarse-grained information rates introduced above have been applied in analysis of EEG recordings of an epileptic patient.

A 30 month old male patient has been suffering from epileptic seizures since the age of 8 months. The Sturge-Weber syndrome has been diagnosed because of congenital periorbital hemangioma and leptomeningeal hemangiomas in the left temporo-occipital area revealed by the magnetic resonance imaging (MRI) scan. His first EEG showed spiking in the left temporo-occipital area. In the beginning he had partial complex seizures; later myoclonic-astatic seizures appeared. Recently, two long-term video/EEG monitoring sessions were performed. The first one showed ictal onset in the left temporal lobe; the second, monitoring by scalp electrodes 1.5 years later, revealed mostly generalized spiking with a slight excess in the right temporo-occipital lobe. Interictal positron emission tomography (PET) showed glucose hypometabolism in the left temporo-occipital lobe. A part of the most recent EEG recordings underwent synchronization analysis using the above CIR's, MCIR, and CTIR's. They were estimated from a 1024-sample moving window (moving step 128 samples, sampling frequency 256 Hz), using four marginal equiquantal bins, $\tau_{min}=\Delta\tau=1$, and $\tau_{max}=50$ samples. Signals from reference and longitudinal (bipolar) montages were analyzed. The latter gave clearer results in establishing directions of information flow, i.e., the drive-response relations using the CTIR. From a segment with a short seizure, signals from the leads T_6O_2 [Fig. 5(a)] and F_4C_4 [Fig. 5(b)] are illustrated here. Before the seizure both $i(T_6O_2)$ and $i(F_4C_4)$ present occasional increases, but they develop independently and the mutual CIR $i(T_6O_2,F_4C_4)$ retains low values [Fig. 5(c)]. At the start of the seizure (time 32 sec) the CIR's and MCIR rise sharply, reflecting an increase of both local synchrony (CIR) and synchronization between different areas of the brain (MCIR). The increased synchrony revealed by the increased information rates could also be indicated by decreased entropy rates or decreased ''dimensional complexity'' measures, e.g., by the correlation dimension. These and related dimensional and entropy measures (correlation integrals) have been used recently for anticipating approaching seizures [18,19]. For evaluating predictive properties of CIR's we do not have enough data yet; thus we proceed to the CTIR to find that in the presented segment $i(F_4C_4|T_6O_2)>i(T_6O_2|F_4C_4)$, i.e., the information flow from T_6O_2 to F_4C_4 dominates over the opposite flow, or the subsystem (brain area) represented by the signal from the lead T_6O_2 (signal T_6O_2 for short) drives that from F_4C_4.

For comparison we present the same analysis of the same signals but from a segments of an interictal (i.e., far from seizures) recording (Fig. 6). Both the CIR's $i(T_6O_2)$ and $i(F_4C_4)$ fluctuate on the same level, although the dependence of the signals measured by $i(T_6O_2,F_4C_4)$ is low [Fig. 6(c)]. The drive-response relation cannot be unambiguously defined, since the CTIR's $i(T_6O_2|F_4C_4)$ and $i(F_4C_4|T_6O_2)$ are either approximately the same or exchange their dominance [Fig. 6(d)]. These results suggest that transients to seizures are characterized by an increasing level of synchronization (both local and between areas) and an asymmetry in information flow emerges or is amplified. Considering the latter we have found that the signal T_6O_2 drove all signals from the right hemisphere and even some signals from the left central and frontal areas. Symmetrically the same has been found about the signal T_5O_1; however, there was no distinction of causality between T_5O_1 and T_5T_3. In fact, the latter drove all the signals as T_5O_1 did. On the other hand, there was no distinction of the information flow direction (although there is a nonzero dependence indicated by the MCIR) between laterally symmetrical leads such as C_3P_3 and C_4P_4, with the one exception—T_5O_1 has been found to drive T_6O_2. This analysis suggests that the primary epilepto-

genic area is the left temporal and occipital region, which drives the rest of the left hemisphere and the right temporal and occipital area, which secondarily drives the rest of the right hemisphere. This is in accordance with MRI and PET scan results. The driving from left temporal/occipital to right central/frontal areas, and the symmetrical one, are probably secondary interactions due to common dynamical components in the signals from the left and right temporal/occipital areas.

V. CONCLUSION

An information-theoretic approach has been introduced to study synchronization phenomena in experimental time series. Its ability to detect synchronization as well as to establish drive-response relations has been demonstrated in a numerical study using data generated by unidirectionally coupled chaotic systems. Preliminary but promising results from analysis of EEG recordings of an epileptic patient have also been presented. Applications of the method have currently been extended to a larger group of epileptic patients with the aims of localization of epileptic foci and anticipation of approaching seizures.

ACKNOWLEDGMENTS

The authors would like to thank P. Pokorný, and acknowledge support from the Ministry of Health of the Czech Republic (Grant IGA No. NF6258-3/2000).

[1] L.M. Pecora, T.L. Carroll, G.A. Johnson, and D.J. Mar, Chaos **7**, 520 (1997).
[2] C. Schäfer, M.G. Rosenblum, J. Kurths, and H.-H. Abel, Nature (London) **392**, 239 (1998).
[3] M. Paluš and D. Hoyer, IEEE Eng. Med. Biol. Mag. **17**, 40 (1998).
[4] S.J. Schiff, P. So, T. Chang, R.E. Burke, and T. Sauer, Phys. Rev. E **54**, 6708 (1996).
[5] M. Le Van Quyen, J. Martinerie, C. Adam, and F.J. Varela, Physica D **127**, 250 (1999).
[6] P. Tass, M.G. Rosenblum, J. Weule, J. Kurths, A. Pikovsky, J. Volkmann, A. Schnitzler, and H.-J. Freund, Phys. Rev. Lett. **81**, 3291 (1998).
[7] J. Arnhold, P. Grassberger, K. Lehnertz, and C.E. Elger, Physica D **134**, 419 (1999).
[8] T.M. Cover and J.A. Thomas, *Elements of Information Theory* (J. Wiley & Sons, New York, 1991).
[9] I.P. Cornfeld, S.V. Fomin, and Ya. G. Sinai, *Ergodic Theory* (Springer, New York, 1982).
[10] K. Petersen, *Ergodic Theory* (Cambridge University Press, Cambridge, 1983).
[11] M. Paluš, Neural Network World **7**, 269 (1997).
[12] M. Paluš, Physica D **93**, 64 (1996).
[13] C.W.J. Granger, Econometrica **37**, 424 (1969).
[14] T. Schreiber, Phys. Rev. Lett. **85**, 461 (2000).
[15] R. Quian Quiroga, J. Arnhold, and P. Grassberger, Phys. Rev. E **61**, 5142 (2000).
[16] M. Paluš, Physica D **80**, 186 (1995).
[17] K. Pyragas, Phys. Rev. E **56**, 5183 (1996).
[18] K. Lehnertz and C.E. Elger, Phys. Rev. Lett. **80**, 5019 (1998).
[19] J. Martinerie, C. Adam, M. Le Van Quyen, M. Baulac, S. Clemenceau, B. Renault, and F. Varela, Nature Med. **4**, 1173 (1998).